

Hierarchy-Aware Fine-Tuning of Vision-Language Models

Jiayu Li^{1*} Rajesh Gangireddy² Samet Akcay² Wei Cheng¹ Juhua Hu¹
¹University of Washington ²Intel

Abstract

Vision-Language Models (VLMs) learn powerful multi-modal representations through large-scale image–text pre-training, but adapting them to hierarchical classification is underexplored. Standard approaches treat labels as flat categories and require full fine-tuning, which is expensive and produces inconsistent predictions across taxonomy levels. We propose an efficient hierarchy-aware fine-tuning framework that updates a few parameters while enforcing structural consistency. We combine two objectives: Tree-Path KL Divergence (TP-KL) aligns predictions along the ground-truth label path for vertical coherence, while Hierarchy-Sibling Smoothed Cross-Entropy (HiSCE) encourages consistent predictions among sibling classes. Both losses work in the VLM’s shared embedding space and integrate with lightweight LoRA adaptation. Experiments across multiple benchmarks show consistent improvements in Full-Path Accuracy and Tree-based Inconsistency Error with minimal parameter overhead. Our approach provides an efficient strategy for adapting VLMs to structured taxonomies.

1. Introduction

Vision-Language Models (VLMs) unify visual perception and language understanding in a single multimodal framework. A typical VLM architecture combines a visual encoder, a language encoder or decoder, and a cross-modal alignment module that creates a shared embedding space for image–text reasoning. These architectures enable zero-shot recognition, visual question answering, and caption generation through large-scale image–text pretraining.

Pretraining provides broad generalization but doesn’t ensure optimal performance on domain-specific tasks. Differences in label structure, data distribution, and visual characteristics require task-adaptive fine-tuning. Fully updating billions of parameters demands substantial GPU memory and training cost. Efficient Fine-Tuning (EFT) methods [3, 6, 10, 11, 13] address this by optimizing a small sub-

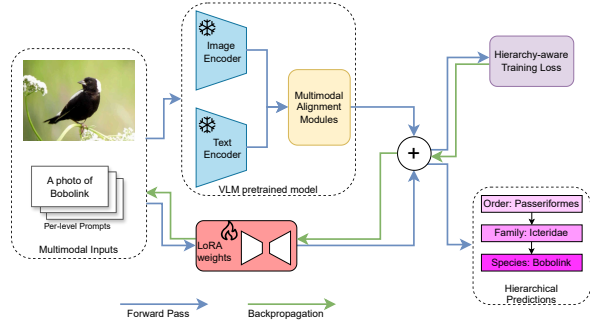


Figure 1. Overview of the proposed hierarchy-aware fine-tuning framework for Vision-Language Models.

set of parameters while keeping pretrained weights frozen. Recent studies show that EFT methods achieve strong performance on visual question answering [19, 36, 45], image captioning [7, 39], cross-modal retrieval [22, 42] and text-guided object detection [23, 31].

VLMs work well for captioning and detection but remain underexplored in hierarchical classification, where labels follow multi-level taxonomies (e.g., order → family → species). Most methods assume a flat label space, ignoring structural dependencies among categories. This produces inconsistent predictions across levels, limiting reliability in fine-grained domains like biodiversity monitoring and medical imaging.

We propose an efficient hierarchy-aware fine-tuning framework for VLMs using Tree-Path KL Divergence (TP-KL) and Hierarchy-Sibling Smoothed Cross-Entropy (HiSCE) losses. TP-KL enforces vertical consistency by matching the predicted label path through the taxonomy with ground truth, while HiSCE encourages horizontal consistency by smoothing probability distributions among sibling classes. Both losses work in the shared image–text embedding space, integrating seamlessly with lightweight EFT methods like LoRA without modifying the pretrained architecture.

Experiments across four hierarchical benchmarks (CUB-200-2011 [37], FGVC-Aircraft [24], Butterfly-200 [5], ChestX-ray14 [40]) show that our approach improves Full

*Work done during Google Summer of Code 2025 with Intel: <https://summerofcode.withgoogle.com/archive/2025/projects/eYkkpBH5>

Path Accuracy (FPA) and reduces Tree-based Inconsistency Error (TICE) compared to standard cross-entropy fine-tuning. Qualitative analysis shows that joint TP-KL + HiSCE optimization produces hierarchy-aligned semantic clusters, improving structural awareness in VLMs.

Our main contributions are:

- The first efficient fine-tuning framework that explicitly models hierarchical label dependencies in VLMs.
- Dual-consistency objectives (TP-KL and HiSCE) that jointly enforce vertical and horizontal consistency across taxonomy levels.
- Comprehensive evaluation across multiple VLM architectures and datasets showing consistent improvements in hierarchy-aware metrics with minimal parameter overhead.

2. Related Work

2.1. Hierarchical Classification

Hierarchical classification investigates visual categorization when labels follow multi-level taxonomies, such as order → family → species in biodiversity datasets or coarse-to-fine disease groupings in medical imaging [2, 8, 30, 44]. Classical methods [18, 34, 46] model the hierarchy explicitly using multi-branch architectures, hierarchical softmax, or structured prediction modules. Recent approaches incorporate hierarchy-awareness through embedding structures, attention mechanisms, and graph-based modeling. [5] introduces coarse-to-fine feature refinement using taxonomy-guided supervision, while [38] enforces vertical path coherence to reduce contradictory predictions across levels. Attention-based models [20] capture cross-level dependencies to improve fine-grained discrimination. Graph-based formulations [8] including hierarchical graph convolution networks and taxonomy-aware GNNs, which propagate semantic information along parent-child edges to enrich label-aware representations. More recent work, such as visually consistent hierarchical image classification [27], aligns feature space geometry with taxonomy structure using contrastive constraints.

However, nearly all previous work relies on unimodal backbones, including EfficientNet-V2 [32] and DeiT-Tiny [33], which achieve strong fine-grained accuracy but lack cross-modal priors from large-scale image–text pretraining. In addition, most methods treat levels independently, which often leads to inconsistent predictions. Our work differs by enforcing both vertical (path-level) and horizontal (sibling-level) consistency directly within a multimodal embedding space of a VLM using customized training loss and smooth labeling.

2.2. Efficient Fine-Tuning of Vision-Language Models

Vision-Language Models (VLMs) leverage large-scale contrastive learning to align images and text in a shared embedding space [16, 17, 29, 41, 43]. While VLMs generalize well in zero-shot settings, adapting them to domain-specific tasks is computationally expensive due to their large number of parameters [15]. Efficient Fine-tuning (EFT) methods, including Prompt Tuning [3, 14], Adapter Tuning [10], LoRA [11], and QLoRA [6], address this challenge by updating only a small subset of parameters while keeping pretrained backbones frozen. Prompt Tuning learns a small set of continuous prompt vectors prepended to the text tokens, guiding the frozen model toward the downstream task with minimal overhead. Adapter Tuning inserts lightweight bottleneck layers inside transformer blocks, allowing task-specific transformations while preserving all pretrained weights. LoRA introduces low-rank decomposition into attention projections, providing memory-efficient weight updates without modifying the original parameters. QLoRA further improves efficiency by quantizing the pretrained backbone to 4-bit while applying LoRA updates on top.

2.3. Hierarchy-Aware Learning in Embedding-Space Models

Taxonomy-aware learning can be achieved through loss-based regularization, which introduces structural priors directly into the optimization objective. Works such as hierarchical attention modeling [12, 20] and hierarchical semantic embedding [5, 25] explore ways to incorporate relationships among parent–child and sibling categories. However, these approaches operate primarily on unimodal embeddings and do not leverage multimodal representations.

The recently proposed Tree-Path KL Divergence [27] enforces global vertical consistency by aligning predicted probability paths with ground-truth label paths, while smoothing-based methods distribute probability mass among semantically related sibling classes. In our work, we extend these ideas into a multimodal embedding space.

3. Methodology

Problem Statement: Given an input image x and its hierarchical labels $\{y^{(1)}, y^{(2)}, \dots, y^{(L)}\}$ across L taxonomy levels, where $y^{(1)}$ denotes the coarsest level with the fewest categories (e.g. order, family, supercategory) and $y^{(L)}$ denotes the finest level with the most categories (e.g. species, variant, specific disease), our goal is to adapt a pretrained vision–language model to produce hierarchy-consistent predictions under efficient fine-tuning constraints.

To explicitly incorporate taxonomy structure into train-

ing, we introduce combining two complementary loss functions: (1) **Hierarchy-Sibling Smoothed Cross-Entropy (HiSCE)** encourages *horizontal* consistency by smoothing the label distribution among sibling classes within the same level, improving robustness against fine-grained misclassifications; and (2) **Tree-Path KL Divergence (TP-KL)** enforces *vertical* consistency by aligning the predicted path across hierarchy levels with the ground-truth taxonomy. The overall training objective combines these components with the standard cross-entropy loss:

$$\mathcal{L}_{total} = \mathcal{L}_{CE} + \lambda_1 \mathcal{L}_{TP-KL} + \lambda_2 \mathcal{L}_{HiSCE},$$

where λ_1 and λ_2 are weights of training loss for TP-KL and HiSCE respectively. The following subsections introduce the details of each component. We later combine TP-KL with HiSCE in Section 4.6 to demonstrate their complementarity.

3.1. Hierarchy-Sibling Smoothed Cross-Entropy Loss (HiSCE)

To enhance intra-level consistency, we apply a loss function called **Hierarchy-sibling Smoothed Cross-Entropy Loss (HiSCE)**. Traditional cross-entropy loss assigns a probability of 1 to the ground-truth label and 0 to all others, which overlooks the semantic similarity among classes under the same parent node. In contrast, our method introduces a hierarchy-aware smoothing mechanism that distributes a small portion of probability to the sibling (or cousin) classes that share the same parent, effectively leveraging structural similarity within each level. We construct a per-level label-smoothing table $T^{(l)}$, where each row corresponds to the smoothed target distribution of one class. Although this table can be viewed conceptually as a list of C_l one-dimensional target vectors, representing each class's softened label distribution, we implement it as a square matrix $T^{(l)} \in \mathbb{R}^{C_l \times C_l}$ for efficient batched indexing in modern deep-learning frameworks.

Formally, the i -th row of $T^{(l)}$ redistributes a small probability mass ε_l uniformly among the siblings of class i , while assigning $1 - \varepsilon_l$ to the diagonal entry as the ground truth. During training, given the ground-truth class index, we retrieve the entire smoothed target vector simply by selecting the corresponding row of $T^{(l)}$.

$$T_{ij}^{(l)} = \begin{cases} 1 - \varepsilon_l, & \text{if } i = j, \\ \frac{\varepsilon_l}{|\mathcal{S}(i)|}, & \text{if } j \in \mathcal{S}(i), \\ 0, & \text{otherwise,} \end{cases} \quad (1)$$

where $\mathcal{S}(i)$ denotes the set of sibling classes of class i .

As shown in Figure 2, HiSCE encourages the model to learn *smooth decision boundaries* within each level of the taxonomy by softly rewarding predictions close to the correct label in semantic space. As a result, the model can

better capture visual and contextual similarities between related categories, improving robustness to fine-grained misclassifications and enhancing hierarchy-consistent generalization.

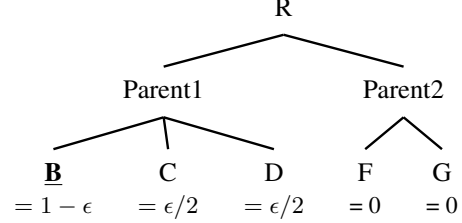


Figure 2. Illustration of hierarchy-sibling smoothing at a single taxonomy level. The ground-truth class **B** retains probability $1 - \varepsilon$, its sibling classes **C** and **D** share the remaining mass ε uniformly, and all non-sibling classes (**F**, **G**) receive 0. This corresponds to one row of the smoothing matrix $T^{(l)}$ in Equation (1).

3.2. Tree-path KL Divergence Loss (TP-KL)

Tree-Path KL Divergence (TP-KL) loss was originally proposed as a model-agnostic approach to enforce *semantic consistency across hierarchy levels*. The key idea is to align the predicted hierarchical path of a sample with its ground-truth label path through the taxonomy. In conventional classification architectures (e.g., CNNs or Transformers), each hierarchy level is equipped with an independent classification head producing logits over classes. TP-KL first concatenates the log-softmax outputs from all levels to form a joint hierarchical distribution and then computes the Kullback–Leibler (KL) divergence between this predicted distribution and the concatenated one-hot ground-truth path.

Formally, given L hierarchy levels, each with logits $z^{(l)}$ and one-hot label vector $\mathbf{1}_{y^{(l)}}$, the TP-KL loss is defined as:

$$Y = \frac{1}{L} [\mathbf{1}_{y^{(L)}}; \dots; \mathbf{1}_{y^{(1)}}] \quad (2)$$

$$\mathcal{L}_{TP-KL} = KL\left(\text{Softmax}([\mathbf{z}^{(L)}; \dots; \mathbf{z}^{(1)}]), Y\right) \quad (3)$$

This loss penalizes predictions that violate the hierarchical structure by encouraging consistent outputs along the tree path from root to leaf nodes.

When applying TP-KL to VLM, the loss formulation remains unchanged; the adaptation lies only in how the prediction distributions are obtained. Instead of using classifier logits from independent heads, VLMs represent categories as *text embeddings* and compute *image–text similarity scores* in a shared embedding space. For each hierarchy level l , the similarity for class c is computed as

$$\mathbf{z}_c^{(l)} = \frac{\mathbf{v}^\top \mathbf{t}_c^{(l)}}{\|\mathbf{v}\| \|\mathbf{t}_c^{(l)}\|} \quad (4)$$

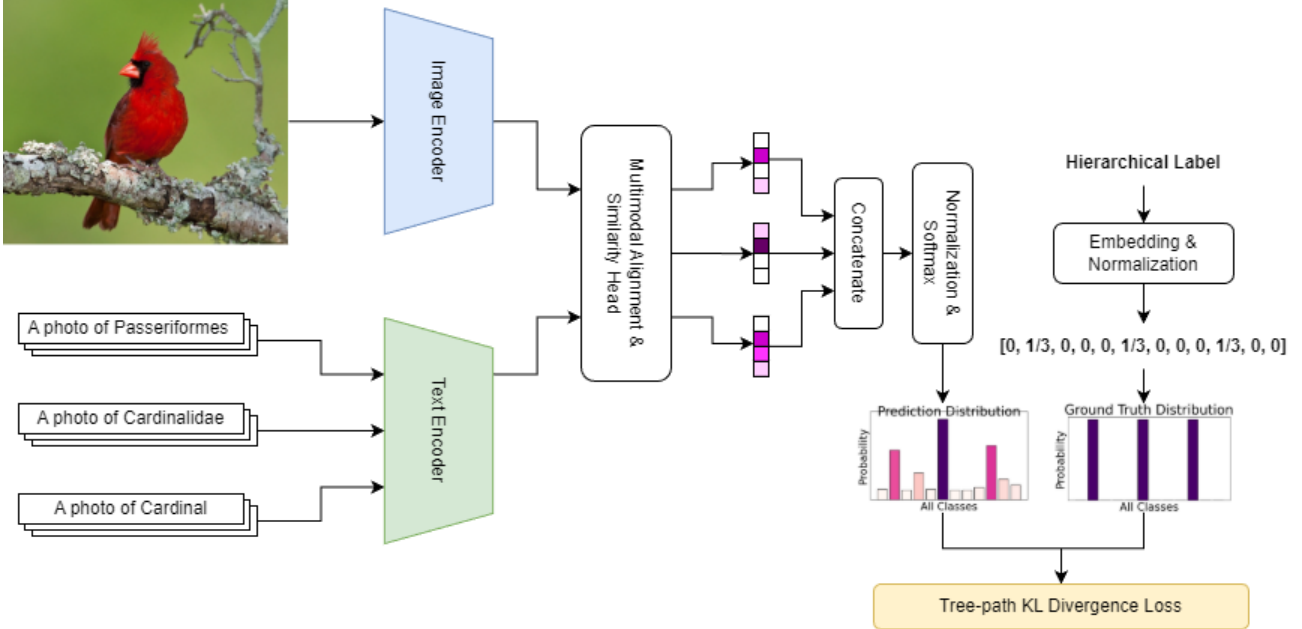


Figure 3. Overview of the Tree-Path KL Divergence computation.

where v and $t_c^{(l)}$ denote normalized image and text embeddings, respectively. The similarity scores of each level are normalized with a temperature-scaled logarithmic softmax [9] and concatenated to form the hierarchical distribution used in the KL divergence. This alignment allows TP-KL to operate directly in the embedding space, making it naturally compatible with EFT strategies such as LoRA or adapter tuning, without altering the original loss formulation.

Figure 3 visualizes how hierarchical predictions from different taxonomy levels are concatenated to form a unified probability path before computing the KL divergence against the ground-truth path distribution. It shows that predictions from all hierarchy levels, e.g., order \rightarrow family \rightarrow species, are first projected into the shared embedding space and then aligned through temperature-scaled log-softmax operations. The resulting joint distribution reflects the complete hierarchical path, enforcing vertical consistency during training.

4. Experiments

We evaluate our hierarchy-aware fine-tuning framework across four datasets with three different model architectures. We first introduce the datasets, then the evaluation metrics, and finally analyze each component.

4.1. Dataset Overview

Table 1 summarizes the hierarchical datasets used for evaluation. These datasets span biodiversity, aviation, and medi-

cal imaging, with hierarchical label structures of two to four taxonomy levels.

CUB-200-2011 [37] is a bird-species benchmark with 11,788 images (5,994 training / 5,794 test). Since the original annotations only provide species-level information, following [4], we add two hierarchy levels (family and order) to create a 3-level label chain: order \rightarrow family \rightarrow species. **FGVC-Aircraft** [24] contains 10,000 aircraft images at three levels: manufacturer, family, and variant. **ChestX-ray14** [40] includes over 112,000 chest X-ray images from 30,000 patients in a three-level disease taxonomy.

Butterfly-200 [5] has \sim 25,000 butterfly images covering 200 species in a four-level hierarchy (family \rightarrow subfamily \rightarrow genus \rightarrow species).

4.2. Evaluation Metrics

We evaluate using accuracy-based metrics and hierarchy-aware consistency metrics.

Accuracy measures the proportion of correctly classified instances at each level, macro-averaged over all levels.

Weighted Average Precision (wAP) [20] assigns greater weight to accuracy at fine-grained levels:

$$\text{wAP} = \sum_{l=1}^L \frac{N_l}{\sum_{k=1}^L N_k} P_l, \quad (5)$$

where N_l and P_l denote the number of classes and precision at level l . wAP emphasizes performance on deeper, fine-grained levels.

Tree-based InConsistency Error rate (TICE) [38]

Dataset	#Class	Hierarchy Label (High → Low)	Levels	Domain
CUB-200-2011 [37]	200	order: 13, family: 38, species: 200	3	Biodiversity
FGVC-Aircraft [24]	100	manufacturer: 30, family: 70, variant: 100	3	Aircraft
ChestX-ray14 [40]	14	supercategory: 3, subcategory: 9, specific disease: 14	3	Medical
Butterfly-200 [5]	200	family: 5, subfamily: 23, genus: 116, species: 200	4	Biodiversity

Table 1. Statistics of hierarchical classification datasets used in our experiments. Each dataset provides multi-level taxonomies ranging from coarse to fine categories.

measures whether the prediction path is valid in the hierarchical tree. $TICE = n_{ic}/N$, where n_{ic} is the number of inconsistent prediction paths and N is the total number of predictions.

Full Path Accuracy(FPA) [27] evaluates overall accuracy and hierarchical consistency. $FPA = n_{ac}/N$, where n_{ac} is the number of samples correct across all hierarchical levels. FPA measures the proportion of instances with entirely correct label paths.

4.3. Baseline Configuration: LoRA-based VLM

We adopt Low-Rank Adaptation (LoRA) [11] as our efficient fine-tuning strategy on CLIP [28].

LoRA introduces lightweight rank-decomposition matrices into linear projection layers of both vision and text transformers. Each weight matrix $W \in \mathbb{R}^{d \times k}$ gets a low-rank update $\Delta W = BA$, where $A \in \mathbb{R}^{r \times k}$, $B \in \mathbb{R}^{d \times r}$. The rank r controls capacity (lower r means fewer trainable parameters), while scaling factor α balances the update magnitude relative to frozen base weights. This reduces GPU memory and fine-tuning cost while maintaining generalization benefits.

We set rank $r = 16$, scaling factor $\alpha = 32$, and dropout $p = 0.3$. Base model weights stay frozen; only LoRA parameters and layer normalization weights are trainable (4.4 million parameters). We use AdamW optimizer [21] with learning rate 1e-3 and train for 100 epochs (Table 2).

Table 2. Experimental Environment Setup

Component	Specification
GPU	NVIDIA RTX 6000
CUDA / Driver	CUDA 13.0 / Driver 581.42
CPU	Intel Xeon Silver 4316 (2.3 GHz)
Memory	128 GB RAM
Operating System	Ubuntu 22.04 LTS
Software	PyTorch 2.3, OTX [26]

Table 3 shows that CLIP-LoRA achieves strong hierarchical classification performance despite few trainable parameters. Compared to fully fine-tuned backbones like EfficientNet-V2 and DeiT-Tiny, CLIP-LoRA shows competitive or superior Full-Path Accuracy (FPA) and hierarchical consistency (TICE) while maintaining high effi-

ciency. These results validate that LoRA tuning preserves VLM generalization and provides a reliable foundation for hierarchy-aware fine-tuning.

4.4. Tree-path KL Divergence Loss

We evaluate Tree-Path KL Divergence (TP-KL) loss on the CLIP-LoRA model (Section 4.3). TP-KL combines with cross-entropy (CE) as

$$L = L_{CE} + \lambda L_{TP-KL} \quad (6)$$

where λ controls hierarchical regularization. We test $\lambda \in \{0, 0.5, 1, 2, 5\}$ across four datasets: CUB-200-2011, FGVC-Aircraft, ChestX-ray14, and Butterfly-200.

Table 4 shows that TP-KL substantially improves Full-Path Accuracy (FPA) and reduces Tree-based Inconsistency Error (TICE) across all domains. Best results use moderate regularization ($\lambda = 2$), with +21.8 FPA and -14.4 TICE on CUB-200-2011, and similar improvements on Butterfly-200 and FGVC-Aircraft. Even on large-scale ChestX-ray14, TP-KL enhances hierarchical consistency while preserving accuracy. Figure 4 shows results across datasets for different λ values.

We also evaluate TP-KL on a conventional vision backbone to show its generality. We fine-tune EfficientNet_v2 with different KL weights ($\lambda = 0, 1, 5$) on CUB-200-2011 and FGVC-Aircraft. Table 5 shows that adding KL improves accuracy and hierarchical consistency, demonstrating that TP-KL benefits conventional vision models too.

4.5. Hierarchy-Sibling Smoothed Cross-Entropy Loss (HiSCE)

We evaluate Hierarchy-Sibling Smoothed Cross-Entropy (HiSCE) on four datasets using CLIP-LoRA (Section 4.3). We compare four configurations:

1. Zero-shot: pretrained CLIP without fine-tuning;
2. CE: fine-tuning with standard cross-entropy;
3. HiSCE: replacing CE with hierarchy-sibling smoothing;
4. CE + HiSCE: combining both with equal weight (1.0).

Table 6 shows that HiSCE consistently enhances Full-Path Accuracy (FPA) and reduces Tree-based Inconsistency Error (TICE) across all datasets. CE + HiSCE achieves best performance, with notable improvements on fine-grained datasets like CUB-200-2011 (FPA: 50.2 → 71.1, TICE:

Table 3. Performance comparison between different configurations.

Architecture	Trainable Params	Dataset	Accuracy	FPA	TICE \downarrow	wAP
EfficientNet_v2 [32]	20.2M	FGVC-Aircraft [24]	71.7	55.7	20.4	71.2
		ChestX-ray14 [40]	59.7	31.7	—	26.6
		CUB-200-2011 [37]	84.3	71.0	—	82.5
		Butterfly-200 [5]	88.4	73.9	—	83.6
deit_tiny [33]	5.6M	FGVC-Aircraft [24]	42.0	21.3	54.9	41.0
		ChestX-ray14 [40]	60.5	31.8	—	28.1
		CUB-200-2011 [37]	61.2	40.0	—	54.8
		Butterfly-200 [5]	76.3	54.3	—	65.1
CLIP-LoRA [29]	4.4M	FGVC-Aircraft [24]	53.0	38.3	17.9	55.0
		ChestX-ray14 [40]	65.8	36.5	11.8	22.9
		CUB-200-2011 [37]	71.7	50.2	21.9	68.8
		Butterfly-200 [5]	83.4	72.1	10.1	79.2

Table 4. Effect of Tree-Path KL Divergence Loss Weights on CLIP-LoRA

Dataset	Metric	CE + $\lambda * KL$				
		$\lambda = 0$	$\lambda = 0.5$	$\lambda = 1$	$\lambda = 2$	$\lambda = 5$
CUB-200-2011 [37]	Accuracy	71.7	81.8	81.7	83.6	81.3
	FPA	50.2	64.9	64.9	72	64.4
	TICE \downarrow	21.9	14.3	14.3	7.5	14.2
	wAP	68.8	75.7	75.8	80.5	75.6
FGVC-Aircraft [24]	Accuracy	53	58	58.1	68.6	58.1
	FPA	38.3	43.8	43.9	61.6	43.9
	TICE \downarrow	17.9	23	22.5	9.8	21.7
	wAP	55	59.1	59.3	72.6	59.9
ChestX-ray14 [40]	Accuracy	65.8	65	66.1	64.9	64.9
	FPA	36.5	45	42.5	45	45.2
	TICE \downarrow	11.8	7.6	7.6	7	7.9
	wAP	22.9	21.5	22.5	25	23.8
Butterfly-200 [5]	Accuracy	83.4	84.7	84.4	86.6	83.7
	FPA	72.1	76.2	76	77.1	75.1
	TICE \downarrow	10.1	6.1	5.8	4.7	6.1
	wAP	79.2	82.3	82.6	83.1	81.2

Table 5. TP-KL on EfficientNet_v2 with different loss weights.

Metric	CUB-200-2011			FGVC-Aircraft		
	$\lambda=0$	$\lambda=1$	$\lambda=5$	$\lambda=0$	$\lambda=1$	$\lambda=5$
Acc.	0.853	0.850	0.858	0.709	0.742	0.764
FPA	0.735	0.724	0.764	0.551	0.593	0.629
wAP	0.836	0.832	0.829	0.705	0.733	0.746

21.9 \rightarrow 6.3). Similar trends appear in Butterfly-200, showing that sibling-level smoothing reinforces semantic coherence within each hierarchy level.

HiSCE complements Tree-Path KL Divergence (TP-KL) by addressing horizontal consistency across sibling categories, while TP-KL enforces vertical path consistency across levels. Together, these objectives provide a comprehensive, lightweight fine-tuning framework for adapting VLMs to structured taxonomies.

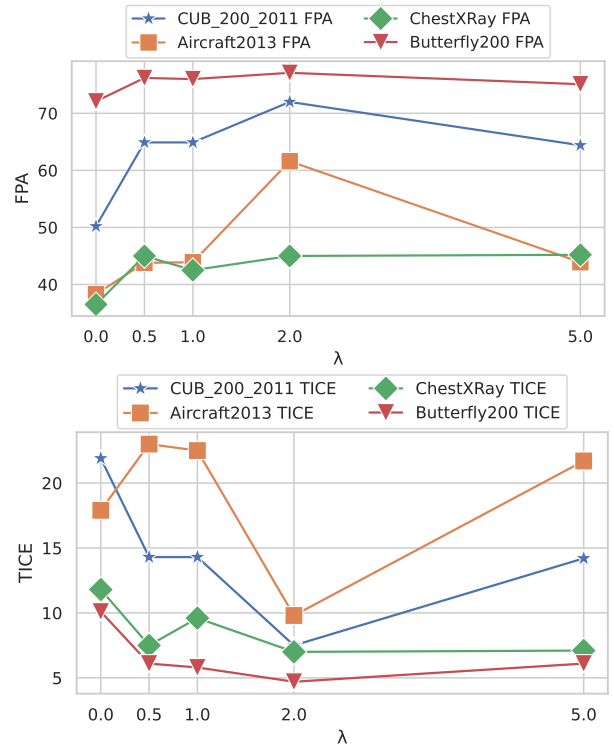


Figure 4. Performance comparison across datasets under different TP-KL weights λ : FPA (top) and TICE (bottom).

4.6. Joint TP-KL and HiSCE Optimization

TP-KL enforces vertical consistency along label hierarchies, while HiSCE promotes horizontal consistency within each level. TP-KL aligns predictions across levels but can over-penalize fine-grained confusion, whereas HiSCE smooths intra-level decisions but lacks global path alignment. We jointly optimize them with base cross-entropy to exploit their complementarity.

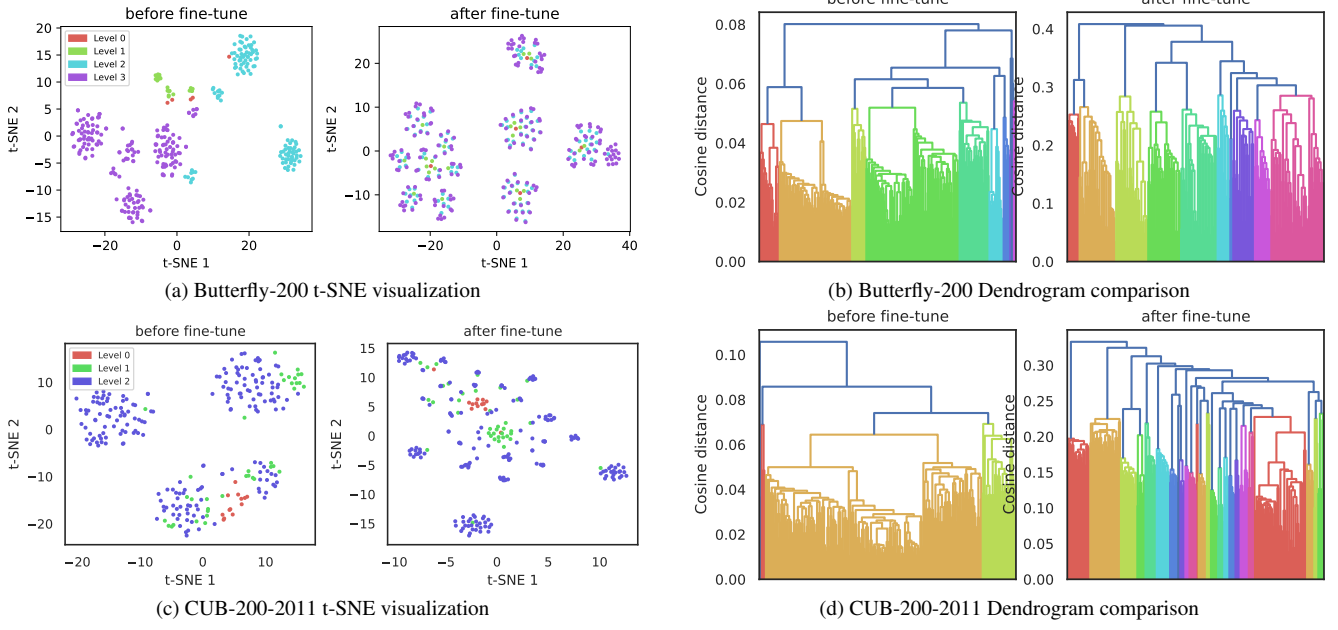


Figure 5. Visualization of text embeddings before and after joint TP-KL + HiSCE optimization on 2 datasets (Butterfly-200 and CUB-200-2011). Left: t-SNE projections, where each point denotes a label embedding colored by its hierarchy level. Right: dendograms visualizing hierarchical grouping, where branch colors indicate clustering structure.

Table 6. Effect of Hierarchy-Sibling Smoothed Cross-Entropy on CLIP-LoRA

Dataset		Zero-shot	CE	HiSCE	CE+HiSCE
CUB-200-2011 [37]	Accuracy	23.4	71.7	81.8	84.1
	FPA	0.5	50.2	63.1	71.1
	TICE \downarrow	98.3	21.9	10.8	6.3
	wAP	44.9	68.8	72.5	79.1
FGVC-Aircraft [24]	Accuracy	19.8	53	49.5	65.1
	FPA	4	38.3	32.7	57
	TICE \downarrow	85.7	17.9	37.5	11.7
	wAP	22.6	55	51.7	70.2
ChestX-ray14 [40]	Accuracy	5.3	65.8	65.5	65.6
	FPA	0	36.5	39.7	43.8
	TICE \downarrow	99.9	11.8	9.1	8.4
	wAP	3.4	22.9	21.7	23.2
Butterfly-200 [5]	Accuracy	13.5	83.4	85	84.7
	FPA	0.8	72.1	77.4	76.5
	TICE \downarrow	84	10.1	3.8	4.9
	wAP	7.9	79.2	82.9	82.2

We use Optuna [1] (100 trials) to find optimal weights λ_1 (TP-KL) and λ_2 (HiSCE) for each dataset, maximizing validation accuracy. Table 7 shows ablation studies comparing individual losses with joint optimization. TP-KL alone causes severe performance drops across datasets, showing that vertical regularization without intra-level smoothing over-penalizes fine-grained errors. HiSCE alone provides strong intra-level consistency but lacks global hierarchical alignment. Joint optimization achieves best results, confirming that vertical (TP-KL) and horizontal (HiSCE) regu-

larization complement each other, yielding hierarchy-aware representations that are both consistent and discriminative.

Table 7. Performance comparison between different configurations.

Dataset	Method	Acc.	FPA	TICE \downarrow	wAP
CUB-200-2011	TP-KL Only	32.1	4.6	29.3	7.9
	HiSCE only	81.8	63.1	10.8	72.5
	Joint	85.1	72.9	5.9	80.6
FGVC-Aircraft	TP-KL Only	12.8	5.6	35.8	10.4
	HiSCE only	49.5	32.7	37.5	51.7
	Joint	69.4	61.5	8.5	73.3
Butterfly-200	TP-KL Only	32.5	13.5	36.7	17.0
	HiSCE only	85	77.4	3.8	82.9
	Joint	87.1	77.5	3.2	82.9
ChestX-ray14	TP-KL Only	67.8	45.5	22.0	20.9
	HiSCE only	65.5	39.7	19.1	21.7
	Joint	67.8	46.2	19.3	16.0

Since all hierarchical levels in CLIP share the same vision encoder output, text embeddings carry hierarchy-specific semantics. Figure 5 visualizes text embeddings before and after fine-tuning using t-SNE projection [35] and hierarchical clustering (dendrogram). Before fine-tuning, label embeddings from different levels (e.g., order, family, species) are scattered and intermixed, showing that pre-trained CLIP doesn't explicitly capture hierarchical dependencies. After joint TP-KL + HiSCE optimization, embeddings show clear multi-level grouping: fine-grained labels

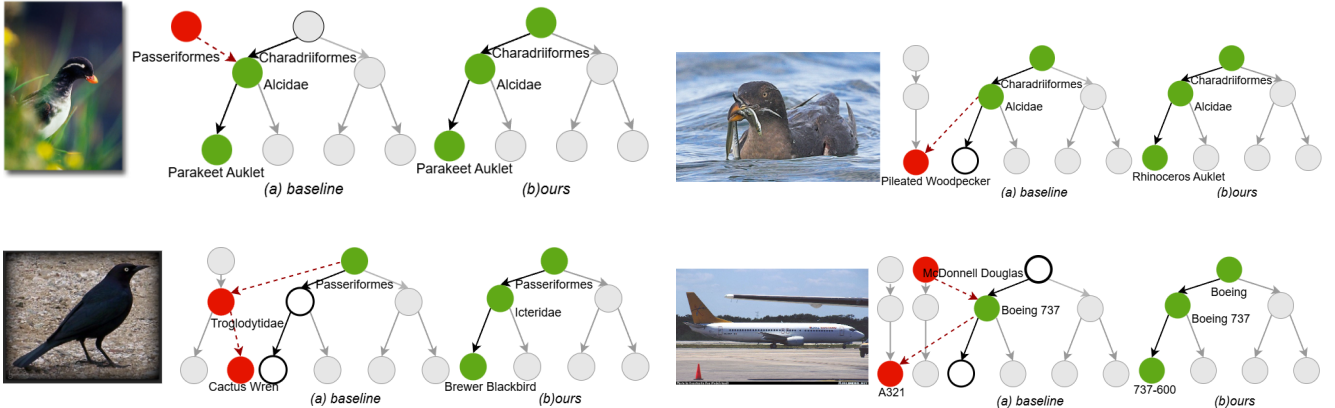


Figure 6. Qualitative comparison of hierarchical predictions between the CLIP-LoRA baseline and our method. Our approach corrects invalid or inconsistent label paths by enforcing vertical and sibling-level consistency across taxonomy levels.

cluster around their coarse-level ancestors, and the structure aligns with ground-truth taxonomy. This confirms that joint objectives encourage the text encoder to internalize hierarchical relationships, transforming the textual embedding space into a semantically consistent manifold. Moreover, Figure 6 illustrates representative prediction examples comparing the CLIP-LoRA baseline with our hierarchy-aware fine-tuning method. While the baseline frequently produces semantically inconsistent label paths that violate parent-child relationships, our approach yields predictions that are coherent across hierarchy levels. By jointly enforcing vertical path alignment and sibling-level consistency, TP-KL and HiSCE reduce error propagation from fine to coarse categories, resulting in more stable and interpretable hierarchical predictions.

5. Conclusion

We introduced an efficient fine-tuning framework for vision-language models on hierarchical classification. Two complementary objectives—Tree-Path KL Divergence (TP-KL) for vertical path consistency and Hierarchy-Sibling Smoothed Cross-Entropy (HiSCE) for horizontal intra-level coherence—enable VLMs to learn taxonomy-consistent representations while updating few parameters. Experiments across four domains show that our approach improves full-path accuracy and reduces hierarchical inconsistency compared to standard cross-entropy, while maintaining LoRA efficiency. Joint TP-KL + HiSCE optimization reshapes the text-embedding space into a hierarchy-aligned manifold, bridging coarse- and fine-grained semantics.

Limitations. Our approach assumes complete and balanced taxonomies, which may limit performance on noisy or sparse hierarchies. We evaluate only on classification tasks, leaving other multimodal settings unexplored.

Future Work. Future directions include handling dynamic or incomplete hierarchies, scaling to open-vocabulary settings, and extending hierarchy-aware objectives to generative or retrieval tasks.

References

- [1] Takuya Akiba, Shohei Sano, Takuma Yanase, Takeru Ohta, and Masanori Koyama. Optuna: A next-generation hyperparameter optimization framework. In *Proceedings of the 25th ACM SIGKDD International Conference on Knowledge Discovery & Data Mining*, pages 2623–2631. ACM, 2019.
- [2] Kim Bjerge, Quentin Geissmann, Jamie Alison, Hjalte MR Mann, Toke T Høye, Mads Dyrmann, and Henrik Karstoft. Hierarchical classification of insects with multitask learning and anomaly detection. *Ecological Informatics*, 77:102278, 2023.
- [3] Tom B. Brown, Benjamin Mann, Nick Ryder, Melanie Subbiah, Jared Kaplan, Prafulla Dhariwal, Arvind Neelakantan, Pranav Shyam, Girish Sastry, Amanda Askell, Sandhini Agarwal, Ariel Herbert-Voss, Gretchen Krueger, Tom Henighan, Rewon Child, Aditya Ramesh, Daniel M. Ziegler, Jeffrey Wu, Clemens Winter, Christopher Hesse, Mark Chen, Eric Sigler, Mateusz Litwin, Scott Gray, Benjamin Chess, Jack Clark, Christopher Berner, Sam McCandlish, Alec Radford, Ilya Sutskever, and Dario Amodei. Language models are few-shot learners, 2020.
- [4] Dongliang Chang, Kaiyue Pang, Yixiao Zheng, Zhanyu Ma, Yi-Zhe Song, and Jun Guo. “Your” flamingo” is my” bird”: Fine-grained, or not. In *Proceedings of the IEEE/CVF conference on computer vision and pattern recognition*, pages 11476–11485, 2021.

[5] Tianshui Chen, Wenxi Wu, Yuefang Gao, Le Dong, Xiaonan Luo, and Liang Lin. Fine-grained representation learning and recognition by exploiting hierarchical semantic embedding. In *Proceedings of the 26th ACM international conference on Multimedia*, pages 2023–2031, 2018.

[6] Tim Dettmers, Artidoro Pagnoni, Ari Holtzman, and Luke Zettlemoyer. Qlora: Efficient finetuning of quantized llms, 2023.

[7] Zhizhao Duan, Hao Cheng, Duo Xu, Xi Wu, Xiangxie Zhang, Xi Ye, and Zhen Xie. Cityllava: Efficient fine-tuning for vlms in city scenario. In *Proceedings of the IEEE/CVF Conference on Computer Vision and Pattern Recognition*, pages 7180–7189, 2024.

[8] Mohannad Elhamod, Kelly M Diamond, A Murat Maga, Yasin Bakis, Henry L Bart Jr, Paula Mabee, Wasila Dahdul, Jeremy Leipzig, Jane Greenberg, Brian Avants, et al. Hierarchy-guided neural network for species classification. *Methods in Ecology and Evolution*, 13(3):642–652, 2022.

[9] Geoffrey Hinton, Oriol Vinyals, and Jeff Dean. Distilling the knowledge in a neural network, 2015.

[10] Neil Houlsby, Andrei Giurgiu, Stanislaw Jastrzebski, Bruna Morrone, Quentin de Laroussilhe, Andrea Gesmundo, Mona Attariyan, and Sylvain Gelly. Parameter-efficient transfer learning for nlp, 2019.

[11] Edward J. Hu, Yelong Shen, Phillip Wallis, Zeyuan Allen-Zhu, Yuanzhi Li, Shean Wang, Lu Wang, and Weizhu Chen. Lora: Low-rank adaptation of large language models, 2021.

[12] Zhihuai Hu, Rihito Kojima, and Xian-Hua Han. Multi-scale attention-driven hierarchical learning for fine-grained visual categorization. *Electronics*, 14(14):2869, 2025.

[13] Zi-Yuan Hu, Yanyang Li, Michael R Lyu, and Liwei Wang. Vi-pet: Vision-and-language parameter-efficient tuning via granularity control. In *Proceedings of the IEEE/CVF International Conference on Computer Vision*, pages 3010–3020, 2023.

[14] Woojeong Jin, Yu Cheng, Yelong Shen, Weizhu Chen, and Xiang Ren. A good prompt is worth millions of parameters: Low-resource prompt-based learning for vision-language models, 2022.

[15] Brian Lester, Rami Al-Rfou, and Noah Constant. The power of scale for parameter-efficient prompt tuning. *arXiv preprint arXiv:2104.08691*, 2021.

[16] Junnan Li, Ramprasaath Selvaraju, Akhilesh Gotmare, Shafiq Joty, Caiming Xiong, and Steven Chu Hong Hoi. Align before fuse: Vision and language representation learning with momentum distillation. *Advances in neural information processing systems*, 34: 9694–9705, 2021.

[17] Junnan Li, Dongxu Li, Caiming Xiong, and Steven C.H. Hoi. Blip: Bootstrapping language-image pre-training for unified vision-language understanding and generation. *arXiv preprint arXiv:2201.12086*, 2022.

[18] Xiaoni Li, Yucan Zhou, Yu Zhou, and Weiping Wang. Mmf: multi-task multi-structure fusion for hierarchical image classification. In *International Conference on Artificial Neural Networks*, pages 61–73. Springer, 2021.

[19] Jiaxiang Liu, Tianxiang Hu, Yan Zhang, Yang Feng, Jin Hao, Junhui Lv, and Zuozhu Liu. Parameter-efficient transfer learning for medical visual question answering. *IEEE Transactions on Emerging Topics in Computational Intelligence*, 8(4):2816–2826, 2023.

[20] Yang Liu, Lei Zhou, Pengcheng Zhang, Xiao Bai, Lin Gu, Xiaohan Yu, Jun Zhou, and Edwin R Hancock. Where to focus: Investigating hierarchical attention relationship for fine-grained visual classification. In *European Conference on Computer Vision*, pages 57–73. Springer, 2022.

[21] Ilya Loshchilov and Frank Hutter. Decoupled weight decay regularization, 2019.

[22] Haoyu Lu, Yuqi Huo, Guoxing Yang, Zhiwu Lu, Wei Zhan, Masayoshi Tomizuka, and Mingyu Ding. Uni-adapter: Unified parameter-efficient transfer learning for cross-modal modeling. *arXiv preprint arXiv:2302.06605*, 2023.

[23] Anish Madan, Neehar Peri, Shu Kong, and Deva Ramanan. Revisiting few-shot object detection with vision-language models. *Advances in Neural Information Processing Systems*, 37:19547–19560, 2024.

[24] Subhransu Maji, Esa Rahtu, Juho Kannala, Matthew Blaschko, and Andrea Vedaldi. Fine-grained visual classification of aircraft, 2013.

[25] Summaya Mumtaz and Martin Giese. Hierarchy-based semantic embeddings for single-valued & multi-valued categorical variables. *Journal of Intelligent Information Systems*, 58(3):613–640, 2022.

[26] Open Edge Platform (Intel). Openvino™ training extensions (otx). https://github.com/open-edge-platform/training_extensions, 2025. Accessed: 2025-10-13.

[27] Seulki Park, Youren Zhang, Stella X. Yu, Sara Beery, and Jonathan Huang. Visually consistent hierarchical image classification, 2025.

[28] Alec Radford, Jong Wook Kim, Chris Hallacy, Aditya Ramesh, Gabriel Goh, Sandhini Agarwal, Girish Sastry, Amanda Askell, Pamela Mishkin, Jack Clark, Gretchen Krueger, and Ilya Sutskever. Learning transferable visual models from natural language supervision, 2021.

[29] Alec Radford, Jong Wook Kim, Chris Hallacy, et al. Learning transferable visual models from natural language supervision. *arXiv preprint arXiv:2103.00020*, 2021.

[30] Rasoul Sali, Sodiq Adewole, Lubaina Ehsan, Lee A Denson, Paul Kelly, Beatrice C Amadi, Lori Holtz, Syed Asad Ali, Sean R Moore, Sana Syed, et al. Hierarchical deep convolutional neural networks for multi-category diagnosis of gastrointestinal disorders on histopathological images. In *2020 IEEE International Conference on Healthcare Informatics (ICHI)*, pages 1–6. IEEE, 2020.

[31] Ahmed Sharshar, Latif U Khan, Waseem Ullah, and Mohsen Guizani. Vision-language models for edge networks: A comprehensive survey. *IEEE Internet of Things Journal*, 2025.

[32] Mingxing Tan and Quoc V. Le. Efficientnetv2: Smaller models and faster training, 2021.

[33] Hugo Touvron, Matthieu Cord, Matthijs Douze, Francisco Massa, Alexandre Sablayrolles, and Herve Jegou. Training data-efficient image transformers & distillation through attention. In *International Conference on Machine Learning*, pages 10347–10357, 2021.

[34] Jack Valmadre. Hierarchical classification at multiple operating points. *Advances in Neural Information Processing Systems*, 35:18034–18045, 2022.

[35] Laurens van der Maaten and Geoffrey Hinton. Visualizing data using t-sne. *Journal of Machine Learning Research*, 9(86):2579–2605, 2008.

[36] Tom Van Sonsbeek, Mohammad Mahdi Derakhshani, Ivona Najdenkoska, Cees GM Snoek, and Marcel Worring. Open-ended medical visual question answering through prefix tuning of language models. In *International Conference on Medical Image Computing and Computer-Assisted Intervention*, pages 726–736. Springer, 2023.

[37] C. Wah, S. Branson, P. Welinder, P. Perona, and S. Belongie. The caltech-ucsd birds-200-2011 dataset. Technical Report CNS-TR-2011-001, California Institute of Technology, 2011.

[38] Rui Wang, Cong Zou, Weizhong Zhang, Zixuan Zhu, and Lihua Jing. Consistency-aware feature learning for hierarchical fine-grained visual classification. In *Proceedings of the 31st ACM International Conference on Multimedia*, pages 2326–2334, 2023.

[39] Tiannan Wang, Wangchunshu Zhou, Yan Zeng, and Xinsong Zhang. Efficientvlm: Fast and accurate vision-language models via knowledge distillation and modal-adaptive pruning. In *Findings of the association for computational linguistics: ACL 2023*, pages 13899–13913, 2023.

[40] Xiaosong Wang, Yifan Peng, Le Lu, Zhiyong Lu, Mohammad Bagheri, and Ronald M Summers. Chestx-ray8: Hospital-scale chest x-ray database and benchmarks on weakly-supervised classification and localization of common thorax diseases. *Proceedings of the IEEE conference on computer vision and pattern recognition (CVPR)*, pages 2097–2106, 2017.

[41] Jinyu Yang, Jiali Duan, Son Tran, Yi Xu, Sampath Chanda, Liqun Chen, Belinda Zeng, Trishul Chilimbi, and Junzhou Huang. Vision-language pre-training with triple contrastive learning. In *Proceedings of the IEEE/CVF conference on computer vision and pattern recognition*, pages 15671–15680, 2022.

[42] Juncheng Yang, Zuchao Li, Shuai Xie, Weiping Zhu, Wei Yu, and Shijun Li. Cross-modal adapter: Parameter-efficient transfer learning approach for vision-language models. In *2024 IEEE International Conference on Multimedia and Expo (ICME)*, pages 1–6. IEEE, 2024.

[43] Jiahui Yu, Zirui Wang, Vijay Vasudevan, Legg Yeung, Mojtaba Seyedhosseini, and Yonghui Wu. Coca: Contrastive captioners are image-text foundation models. *arXiv preprint arXiv:2205.01917*, 2022.

[44] Zhen Yu, Toan D Nguyen, Lie Ju, Yaniv Gal, Maithili Sashindranath, Paul Bonnington, Lei Zhang, Victoria Mar, and Zongyuan Ge. Hierarchical skin lesion image classification with prototypical decision tree. *npj Digital Medicine*, 8(1):26, 2025.

[45] Jinxu Zhang, Yongqi Yu, and Yu Zhang. Cream: coarse-to-fine retrieval and multi-modal efficient tuning for document vqa. In *Proceedings of the 32nd ACM International Conference on Multimedia*, pages 925–934, 2024.

[46] Xinqi Zhu and Michael Bain. B-cnn: branch convolutional neural network for hierarchical classification. *arXiv preprint arXiv:1709.09890*, 2017.